

# Polypropylene nucleation on a glass fibre after melt shearing

B. MONASSE

*Centre de Mise en Forme des Matériaux, Ecole Nationale Supérieure des Mines de Paris, Unité de Recherche Associée au CNRS 1374, Sophia-Antipolis, 06565 Valbonne Cédex, France*

Thermoplastic composites may exhibit a wide range of crystalline morphologies in the neighbourhood of fibres. It was found that glass fibre shearing of a molten polypropylene at high temperature modifies the subsequent isothermal crystallization ( $T_c = 122^\circ\text{C}$ ) under static conditions. The crystallization results have been analysed as a function of the previous high temperature, shear,  $\gamma$ , shear rate,  $\dot{\gamma}$ , and shear stress,  $\tau$ . The mechanical parameters at high temperature,  $\gamma$ ,  $\dot{\gamma}$ ,  $\tau$ , have been calculated for two shearing temperatures ( $T = 170, 210^\circ\text{C}$ ) and two fibre displacements. An  $\alpha$ -phase nucleation process took place at the fibre surface after shearing at the higher temperature ( $T = 210^\circ\text{C}$ ). The nucleation increased with shear but did not appear for static conditions. A strong nucleation process in  $\beta$  phase appeared on the fibre surface after shearing of the polymer at the lower temperature ( $T = 170^\circ\text{C}$ ). These strong morphological modifications with shearing temperature have been analysed as a function of mechanical and thermodynamical parameters.

## 1. Introduction

The mechanical properties of thermoplastic composites are defined by the properties of the material components, the shape, orientation and amount of fibres, and by the fibre-matrix interface [1]. The crystalline structures and morphologies of the matrix may depend on its interaction with fibres. This interaction, critical for the mechanical coupling between matrix and fibres, can be revealed by the crystalline morphology near the fibres.

Isotactic polypropylene is very widely used as a matrix for glass-fibre composites transformed by stamping and injection-moulding processes. Three crystalline phases are known for isotactic polypropylene:  $\alpha$  monoclinic phase [2],  $\beta$  hexagonal phase [3] and  $\gamma$  triclinic phase [4]. The triclinic  $\gamma$  phase has been observed during slow cooling crystallization under high pressure [5] or using low molecular weight polypropylenes [4]. Usually, isotactic polypropylene crystallizes in the  $\alpha$ -phase from the melt. It is the most thermodynamically stable phase [6]. The birefringence of  $\alpha$ -phase spherulites is positive or negative depending on crystallization temperature [7]. These spherulites are easily distinguished from  $\beta$ -phase spherulites revealed by a very strong negative birefringence [7]. The metastable  $\beta$ -phase [3] crystallizes from the melt in the  $105\text{--}135^\circ\text{C}$  range [8]. Several experimental parameters favour  $\beta$ -phase crystallization: a thermal gradient [9], shearing [10] or elongation [11] of the polymer melt during crystallization and nucleating agents in the polymer [12].

Several papers [13, 14] have mentioned a strong  $\alpha$ -phase nucleation on glass fibres when the poly-

propylene is sheared by the fibre displacement during crystallization. This strong surface nucleation is also observed on glass fibres whatever their location in injection-moulded composites [13]. It must be noticed that only part of the polymer crystallizes during the filling stage of the injection-moulding process. The main part of the polymer crystallizes in quasi-static conditions but the morphologies in contact with fibres are quite similar to those appearing during the filling stage. The aim of the present work was to prove that the static crystallization of a thermoplastic composite can be strongly modified by a previous high-temperature shearing induced by the fibre.

## 2. Experimental procedure

High temperature shearing and subsequent static crystallization were applied to a polypropylene in a hot stage, the polypropylene was then observed under an optical microscope.

### 2.1. Materials

The polypropylene homopolymer used was supplied under the reference 3120 MN 1 ( $\overline{M}_n = 39\,400$ ,  $\overline{M}_w = 212\,000$ ,  $\overline{M}_w/\overline{M}_n = 5.4$ ). Each individual glass fibre coated with an unsaturated polyester (5–15 cm long,  $17\ \mu\text{m}$  diameter) was pulled out of a mesh of 100 identical fibres.

### 2.2. Methods

The temperature of the Mettler FP 52 hot stage was

calibrated with benzoic acid (melting temperature  $T_m = 122.35^\circ\text{C}$ ) and anisic acid ( $T_m = 182.98^\circ\text{C}$ ) under isothermal conditions. The crystallization was observed with a Reichert Zetopan POL optical microscope under polarized light.

Two steps were necessary to obtain the composite material: preparation of solid polypropylene films and incorporation of a glass fibre between two identical films, 2–3 cm long. The composite was obtained by melting the polymer at  $210^\circ\text{C}$  between two glass plates approximately  $250\ \mu\text{m}$  apart and then crystallizing by cooling to room temperature. This procedure strongly reduces polymer shearing during the preparation of the composite and ensures fibre location in the middle of the piece all along the sample.

Identical composites were thus prepared: each was used for only one experiment ending in an isothermal crystallization ( $T_c = 122^\circ\text{C}$ ). The thermomechanical treatment in the melt is defined by the temperature,  $T$ , the fibre speed,  $V_T = 2\ \text{mm s}^{-1}$ , and the fibre displacement,  $L_T$ . Then the polymer was cooled to the crystallization temperature,  $T_c = 122^\circ\text{C}$ , at a constant rate,  $dT/dt = \dot{T} = -10^\circ\text{C min}^{-1}$ , without any further displacement of the fibre. Fig. 1 summarizes the procedure used to study isothermal crystallization under static conditions after high-temperature shearing of the polymer.

Five experimental conditions were applied: four experiments with high-temperature shearing applied by a  $2\ \text{mm s}^{-1}$  fibre speed (B–E, Table I) and a reference experiment under static conditions, throughout the whole experiment (A, Table I).

### 3. Results

The morphologies were observed from the beginning of isothermal crystallization  $T_c = 122^\circ\text{C}$ . The morphologies growing from the fibre surface and in the vicinity of the fibre were carefully analysed and com-

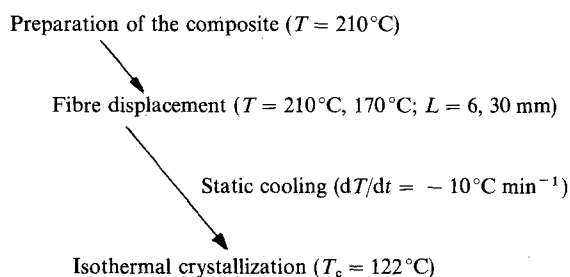


Figure 1 Experimental procedure.

TABLE I Thermo-mechanical parameters applied to the molten composite at high temperature

Experiment	Displacement (mm)	
	170°C	210°C
A		0
B		6
C		30
D	6	
E	30	

pared to those appearing far from the fibre, i.e. at a distance of more than  $20\ \mu\text{m}$  (Fig. 2).

The experiment (A, Figure 2a) with only a static thermal treatment exhibited no specific nucleation process at the fibre surface or in its vicinity, compared with the whole sample. The spherulites nucleated far from the fibre always grew into the monoclinic  $\alpha$ -phase. This implies that a thermal treatment without shearing at any stage of the procedure does not induce a surface nucleation on this glass fibre.

A previous shearing at high temperature,  $T = 210^\circ\text{C}$ , modified the static crystallization near the fibre (B, C, Fig. 2b, c). Many  $\alpha$  spherulites grew from the fibre surface, the glass fibre acting as a nucleating surface. The nuclei seemed to be regularly spaced along the fibre. Their mean distance along the fibre decreased with increasing displacement imposed to the fibre at a constant speed,  $V_T = 2\ \text{mm s}^{-1}$ , at  $T = 210^\circ\text{C}$ : 20 or  $50\ \mu\text{m}$  mean distance between nuclei after a 30 or 6 mm displacement, respectively (Figure 2b, c).

The morphologies formed on the fibre surface were very different when the shearing was applied at  $170^\circ\text{C}$ . A columnar growth in  $\beta$  phase was induced from the fibre surface, producing a transcrystalline morphology. The columnar growth resulted from a strong nucleation on the fibre surface which drastically reduced the lateral growth of spherulites. The strong surface nucleation did not seem to be affected by the amplitude of the previous fibre displacement (Fig. 2d, e). The growth of the  $\beta$  transcrystalline zone was stopped only by the impingement with  $\alpha$ -phase spherulites nucleated far from the surface (Fig. 2d, e). The nucleation of these  $\alpha$ -phase spherulites was only slightly increased by previous shearing of the polymer at  $170^\circ\text{C}$ .

Consequently, previous shearing of the polymer at high temperature strongly modifies the crystallization on the fibre surface but only slightly far away from the fibre.

### 4. Thermomechanical model

The axial movement of the fibre induces polymer shearing, defined by the shear rate with a cylindrical symmetry and without end effect along the fibre (Fig. 3)

$$\dot{\gamma} = -\frac{dV_z}{dr} \quad (1)$$

where  $V_z$  is in cylindrical coordinates, the component of the polymer velocity in the direction of the fibre axis ( $z$ -axis),  $r$  is the radial transverse coordinate. Then, the shear

$$\gamma = \int_0^r \dot{\gamma} dt \quad (2)$$

and the shear stress

$$\tau = \eta \dot{\gamma} \quad (3)$$

can be defined. A power law is assumed to describe viscosity

$$\eta = m(T) \dot{\gamma}^{n-1} \quad (4)$$

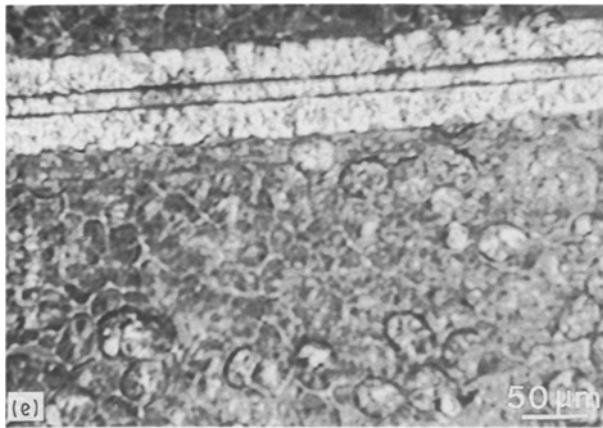
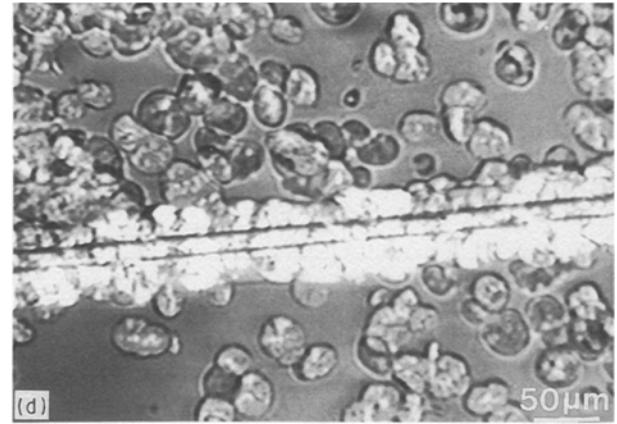
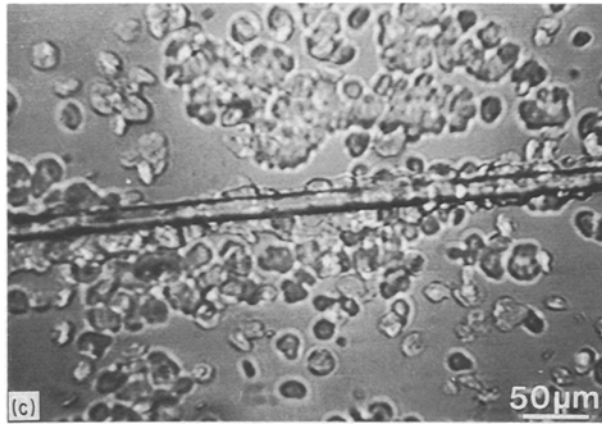
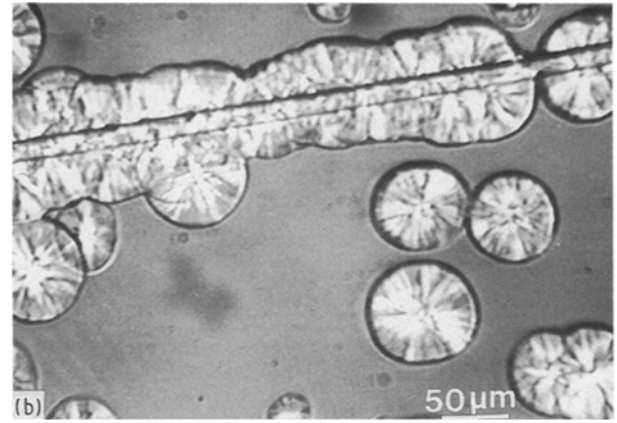
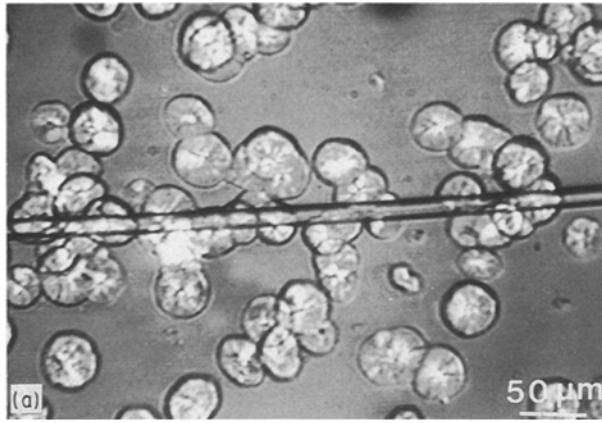


Figure 2 (a) Static crystallization without shearing. (b) Static crystallization after a 6 mm displacement of the fibre at 210 °C. (c) Static crystallization after a 30 mm displacement of the fibre at 210 °C. (d) Static crystallization after a 6 mm displacement of the fibre at 170 °C. (e) Static crystallization after a 30 mm displacement of the fibre at 170 °C.

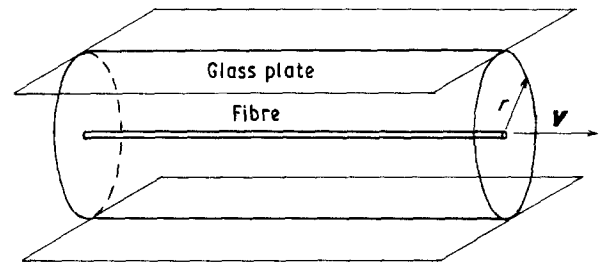


Figure 3 Geometrical definition of the shear experiment.

The shear rate and shear stress are deduced from the force balance equation

$$\eta \frac{\partial V_z}{\partial r} + \frac{\partial \eta}{\partial r} \frac{\partial V_z}{\partial r} + \eta \frac{\partial^2 V_z}{\partial r^2} = 0 \quad (5)$$

With the viscosity power law, this equation reduces to

$$\frac{\partial \dot{\gamma}}{\dot{\gamma}} = - \frac{\partial r}{r} \quad (6)$$

Integration of this equation with the following boundary conditions ( $V_z = V_f$  for  $r = r_f$ ,  $V_z = 0$ , for  $r = r_e$ ) implies

$$\dot{\gamma} = \frac{1-n}{n} \frac{1}{r^{1/n}} \left[ \frac{1}{r_f^{1-1/n} - r_e^{1-1/n}} \right] V_f \quad (7)$$

where  $r_e$  and  $r_f$  are the external and fibre radii,  $r$  is the location in the polymer ( $r_f \leq r \leq r_e$ ) and  $n$  is the exponent in the viscosity power law equation. Con-

sequently, the shear stress is

$$\begin{aligned} \tau &= \eta \dot{\gamma} \\ &= \frac{m}{r} \left[ \left( \frac{1-n}{n} \right) V_f \frac{1}{r_f^{1-1/n} - r_e^{1-1/n}} \right]^n \end{aligned} \quad (8)$$

The rheological parameters measured at 210 and 190 °C by capillary rheometry on polypropylene [15] were extrapolated to 170 °C (Table II).

The mechanical model predicts a strong decrease in the velocity along the radius from the surface (Fig. 4). This decrease mainly results from the value of the power-law exponent,  $n$  (Fig. 5, Equation 7). A very strong shear strain at the glass-fibre surface ( $\dot{\gamma} > 380 \text{ s}^{-1}$ ) results from the shape of the velocity field. It also implies a strong decrease of the shear rate

TABLE II Rheological data of polypropylene

	Temperature (°C)	
	170	210
$m$ (Pa s <sup>-n</sup> )	20 000	7380
$n$	0.35	0.38

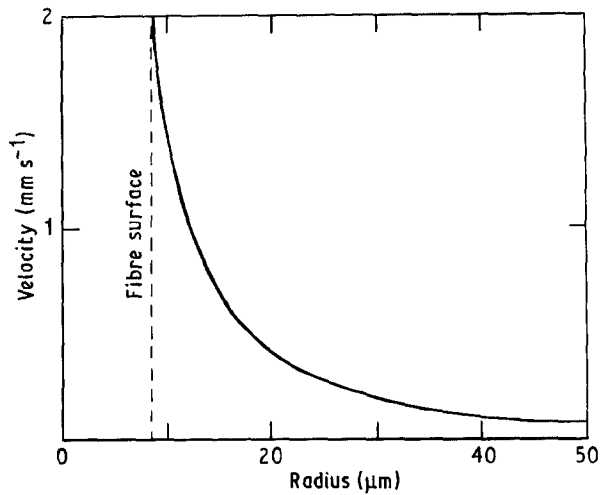


Figure 4 Prediction of the velocity,  $V_z$ , along the radius  $r$  ( $n = 0.35$ ).

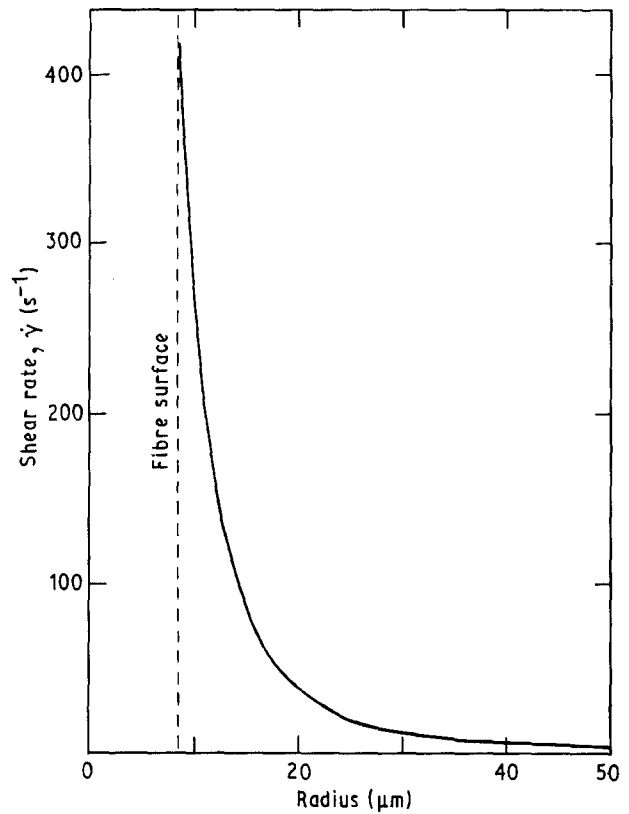


Figure 6 Prediction of the shear rate along the radius  $r$  ( $n = 0.35$ ).

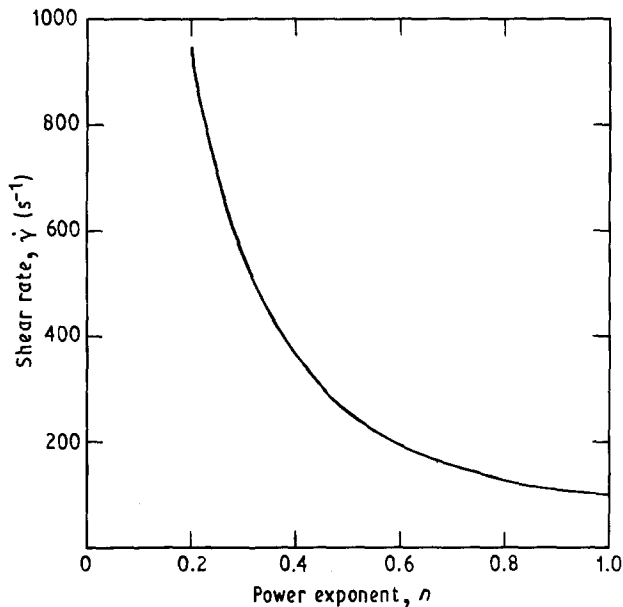


Figure 5 Effect of the power-law exponent,  $n$ , on the shear rate value at the fibre surface.

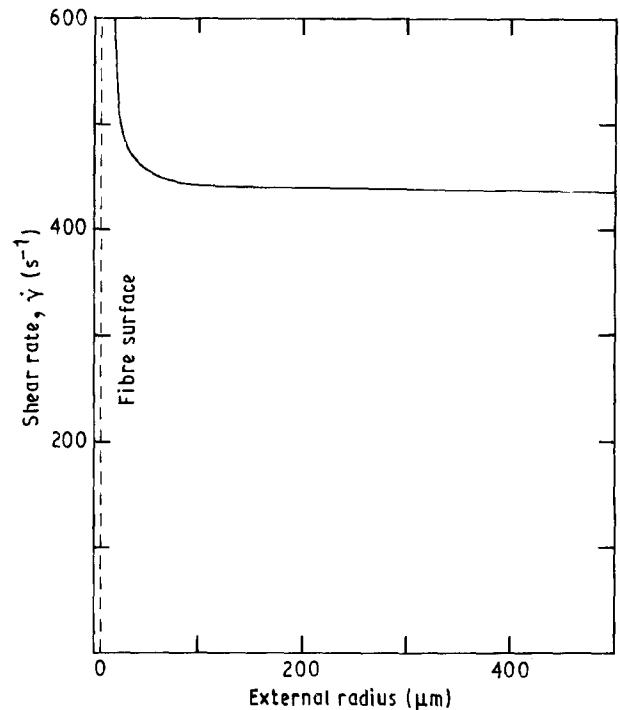


Figure 7 Effect of the outer surface location on the maximum shear rate at the fibre surface ( $n = 0.35$ ).

along the radius: 20  $\mu\text{m}$  is sufficient to lower the shear rate from about  $\dot{\gamma} = 400 \text{ s}^{-1}$  to  $\dot{\gamma} = 20 \text{ s}^{-1}$  (Fig. 6). This result is only slightly modified when the external surface is closer than 100  $\mu\text{m}$  to the fibre surface (Fig. 7). This high insensitivity of the results to the location of the outer surface justifies the cylindrical approximation used to derive this analytical model. For the same reason, the shear stress is the highest at the fibre surface and strongly decreases along the radius (Fig. 8).

This high value and strong variation of shear rate come from the geometry of contact (cylinder) and from the exponent,  $n$ , of the rheological law. The change

between 170 and 210  $^{\circ}\text{C}$  in the maximum shear rate results only from the value of the power law exponent of polypropylene (Fig. 5). The maximum shear is easily deduced from the knowledge of the shear rate and experiment duration  $\gamma = \dot{\gamma}t$ . The shear values are  $\gamma = 1315$  and 6576 for 6 and 30 mm displacements at 170  $^{\circ}\text{C}$ , respectively. These values do not consider polymer relaxation during polymer shearing and during cooling to the crystallization temperature. The

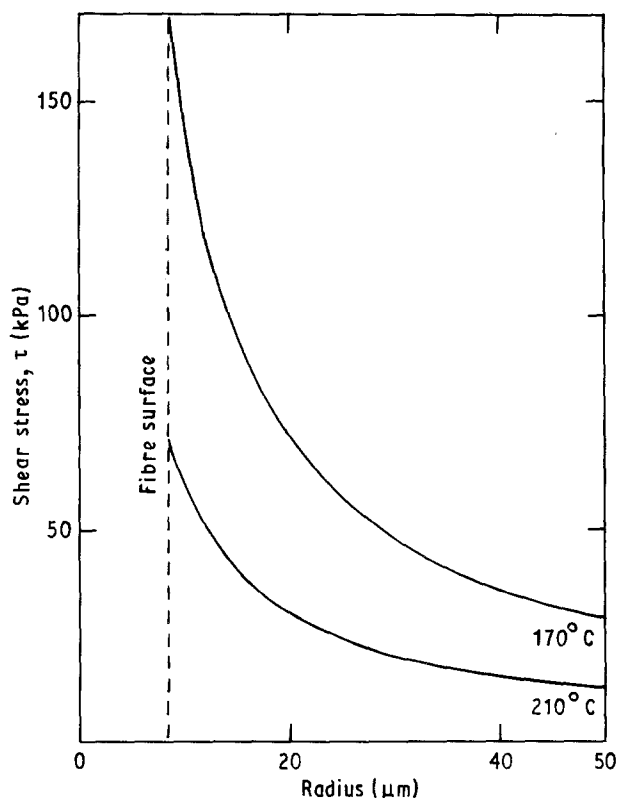


Figure 8 Shear stress change along the radius at two reference temperatures ( $T = 170$  and  $210^\circ\text{C}$ ).

final result of the mechanical model is that the shear stress strongly decreases when the shear temperature increases as an effect of thermal dependence of viscosity (Fig. 8).

## 5. Discussion

The crystallization data have been analysed as a function of shear rate,  $\dot{\gamma}$ , shear,  $\gamma$ , and shear stress,  $\tau$ . The maximum values of all these mechanical parameters are located at the fibre surface. Consequently, it becomes obvious that the shearing effect on crystallization must appear on the fibre surface as observed.

These crystallization effects of shear are located only on the fibre surface as a result of the strong decrease of the shear parameters along the radius. Only  $20\ \mu\text{m}$  is necessary to decrease the shear rate by 90% and the shear stress by 50%. The results are discussed to ascertain if either the shear rate,  $\dot{\gamma}$ , or the shear stress effectively act on nucleation and crystalline growth.

Shear experiments at  $210^\circ\text{C}$  induce a low nucleation effect on the fibre surface in spite of the high shear rate,  $\dot{\gamma} = 386\ \text{s}^{-1}$ . The combination of relaxation during shear and during the composite cooling can explain the weakness of the surface nucleation. To reach the crystallization temperature, 8 min 48 s are necessary at a  $10^\circ\text{C min}^{-1}$  cooling rate. Such a duration is sufficient to relax most of the polymer orientation and, consequently, the shear effect on crystallization. Most of the relaxation must appear at high temperature as an effect of the decrease of relaxation time with temperature. This temperature is very close to the equilibrium melting temperature ( $T_m^0 = 208^\circ\text{C}$ ) [16] and the activation of stable nuclei is highly

improbable. In spite of this relaxation, the shear,  $\gamma$ , modifies the nucleation process, mainly increasing the density of surface nuclei (Fig. 2b, c). The use of shear experiments at one temperature is not sufficient to conclude that nucleation effects the shear rate or shear stress.

The strong  $\beta$  nucleation on the fibre surface observed after a  $170^\circ\text{C}$  shearing is strongly different from the weak  $\alpha$  nucleation observed after a  $210^\circ\text{C}$  shearing. The model predicts very similar shear rates on the fibre surface under these two thermal conditions. On the other hand, the shear stress decreases from 168.1 kPa to 70.9 kPa when the temperature changes from  $170^\circ\text{C}$  to  $210^\circ\text{C}$ . From a mechanical point of view, the shear stress seems to be the significant parameter which controls the surface nucleation on the fibre. Moreover, the shearing temperature,  $T = 170^\circ\text{C}$ , is below the equilibrium melting temperature of the  $\alpha$ -phase ( $T_{m\alpha}^0 = 208^\circ\text{C}$ ) and near the  $\beta$ -phase ( $T_{m\beta}^0 = 170^\circ\text{C}$ ) [17].

Consequently,  $\alpha$ - or  $\beta$ -phase nuclei could be activated under shearing below the equilibrium melting temperature. According to this hypothesis, it is interesting to observe that only  $\beta$ -phase nuclei are activated under shearing at  $170^\circ\text{C}$  and not the  $\alpha$ -phase nuclei (Fig. 2). This observation indicates that stable  $\beta$ -phase nuclei are activated under  $170^\circ\text{C}$  shearing. This hypothesis also explains why so large a number of  $\beta$ -phase nuclei are activated but not why only the  $\beta$ -phase nuclei appear.

## 6. Conclusion

Surface nucleation on a glass fibre highly depends on polymer shearing previously applied at high temperature. This effect observed during isothermal crystallization under static condition depends on shear rate and shearing temperature. High shear rate and shear stress result from axial fibre movement which strongly localizes the nucleation effect on the fibre surface. The nuclei density and the crystalline phase on the fibre surface greatly depend on shearing temperature. Stable crystalline nuclei seem to be activated under shearing provided that the shear temperature is below the equilibrium melting temperature of the crystalline phase and no temperature-dependent degradation occurs. By this method it is possible to change the crystalline morphology of the polymeric matrix in contact with the fibre and to check this effect on the mechanical properties of the composite without any modification of the fibre coating.

## References

1. S. H. MORRELL, *Plast., Rubb. Process. Appl.* **1** (1981) 179.
2. G. NATTA, P. CORRADINI and M. CESARI, *Nuovo Cimento Rend.* **21** (1956) 356.
3. D. R. MORROW, *J. Macromol. Sci. Phys.* **B3**(1) (1969) 53.
4. E. J. ADDINK and J. BEINTEMA, *Polymer* **2** (1961) 185.
5. K. D. PAE, D. R. MORROW and J. A. SAUER, *Nature* **211** (1966) 514.
6. G. NATTA and P. CORRADINI *Nuovo Cimento Suppl.* **15** (1960) 40.
7. F. J. PADDEN and H. D. KEITH, *J. Appl. Phys.* **30** (1959) 1479.

8. J. VARGA, *J. Thermal Anal.* **31** (1986) 165.
9. A. J. LOVINGER, J. O. CHUA and C. C. GRYTE, *J. Polym. Sci. Polym. Phys. Ed.* **15** (1977) 641.
10. D. R. FITCHMUN and Z. MENCIK *ibid.* **11** (1973) 951.
11. H. J. LEUGERING and G. KIRSCH, *Angew. Makromol. Chem.* **33** (1977) 17.
12. A. DUSTWALT and W. W. COX, *Amer. Chem. Soc. Div. Org. Coat.* **30** (1970) 93.
13. A. MISRA, B. L. DEOPURA, S. F. XAVIER, F. D. HARTLEY, R. H. PETERS, *Angew. Makromol. Chem.* **113** (1983) 113.
14. M. J. FOLKES and S. T. HARDWICK, *J. Mater. Sci. Lett.* **3** (1984) 1071.
15. C. TZOGANAKIS, J. VLACHOPOULOS, A. E. HAMIELEC and D. M. SHINOZAKI, *Polym. Engng. Sci.* **29**(6) (1989) 390.
16. B. MONASSE and J. M. HAUDIN, *Colloid Polym. Sci.* **263** (1985) 822.
17. R. J. SAMUELS, *J. Polym. Sci. Polym. Phys. Ed.* **13** (1975) 1417.

*Received 27 June 1991  
and accepted 7 February 1992*